

A New Angle on Pluronic Additives: Advancing Droplets and Understanding in Digital Microfluidics

Sam H. Au,^{†,‡} Paresh Kumar,[§] and Aaron R. Wheeler^{*,†,‡,⊥}

[†]Institute for Biomaterials and Biomedical Engineering, University of Toronto, 164 College Street, Toronto, ON, M5S 3G9

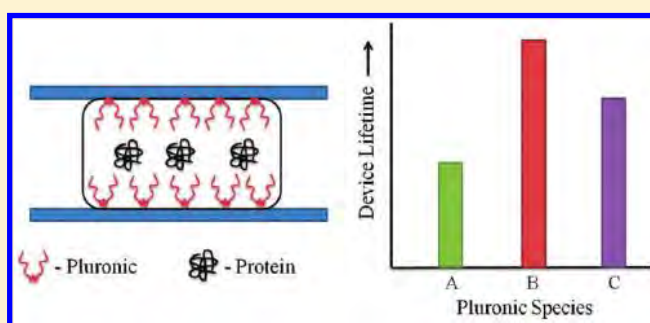
[‡]Donnelly Centre for Cellular and Biomolecular Research, 160 College Street, Toronto, ON, M5S 3E1

[§]Department of Electrical Engineering, Indian Institute of Technology Madras, Chennai–600 036, TN, India

[⊥]Department of Chemistry, University of Toronto, 80 St. George Street, Toronto, ON, M5S 3H6

S Supporting Information

ABSTRACT: Biofouling in microfluidic devices limits the type of samples which can be handled and the duration for which samples can be manipulated. Despite the cost of disposing fouled devices, relatively few strategies have been developed to tackle this problem. Here, we have analyzed a series of eight amphiphilic droplet additives, Pluronic copolymer of poly(propylene oxide) (PPO) and poly(ethylene oxide) (PEO), as a solution to biofouling in digital microfluidics using serum-containing cell culture media as a model fluid. Our analysis shows that species with longer PPO chains are superior for enabling droplet motion and reducing biofouling. Two of the tested species, L92 and P105, were found to lengthen device lifetimes by 2–3 times relative to additives used previously when used at optimal concentrations. Pluronics with low PEO content such as L92 were found to be cytotoxic to an immortalized mammalian cell line, and therefore we recommend that Pluronic additives with greater or equal to 50% PEO composition, such as P105, be used for digital microfluidic applications involving cells. Finally, contact angle measurements were used to probe the interaction between Pluronic-containing droplets and device surfaces. Strong correlations were found between various types of contact angle measurements and the capacity of additives to reduce biofouling, which suggests that contact angle measurements may be useful as a tool for rapidly screening new candidates for the potential to reduce biofouling. We propose that this study will be useful for scientists and engineers who are developing digital microfluidic platforms for a wide range of applications involving protein-containing solutions, and in particular, for applications involving cells.



INTRODUCTION

Biofouling, or unwanted adsorption of biomolecules to surfaces, is a serious problem for a wide range of applications including implanted medical devices, bioreactors, and filtration membranes.^{1–5} Biofouling is exacerbated in microfluidic devices because of the high surface area to volume ratios in these systems. A number of strategies exist to combat fouling in channel-based microfluidics,^{6–10} yet few strategies have been developed to prevent fouling in digital microfluidic (DMF) systems. Here, we build upon our previous work¹¹ to develop a strategy for minimizing fouling caused by the use of protein solutions (with a special emphasis on cell culture media) to maximize the lifetime of DMF devices.

Digital microfluidics is a fluid-handling technique in which droplets are manipulated on an open surface by applying electrical potentials to an array of electrodes embedded underneath an insulator.¹² Because of its ability to precisely dispense, mix, merge, and split discrete droplets, DMF is becoming an increasingly popular tool for biological and biochemical applications,¹³ including cell-based assays,^{14–17} enzyme assays,^{18–21} immunoassays,^{22–24} processing of samples for proteomic analysis,^{25–30} applications

involving DNA,^{31–33} and clinical sample processing and analysis.³⁴ DMF device surfaces are typically coated with a fluorinated polymer such as Teflon-AF;²⁸ unfortunately, these types of surfaces are susceptible to unwanted protein adsorption.^{35,36} This is particularly problematic for digital microfluidics; when proteins adsorb and accumulate, the hydrophobic device surface becomes hydrophilic, which slows and eventually stops aqueous droplet motion, resulting in reduced device lifetimes. Cell culture media is particularly challenging for DMF; the biofouling caused by high concentrations of serum (a complex mixture of proteins and other factors) in such solutions makes droplets immobile on many kinds of DMF devices.

Previous strategies for reducing the amount of protein adsorption to surfaces of digital microfluidic devices include immersion in water-immiscible oils,³⁷ careful modulation of applied voltage polarities,³⁸ the use of replaceable plastic films,³⁹ and operation

Received: March 31, 2011

Revised: May 16, 2011

Published: June 09, 2011

on superhydrophobic surfaces.^{40,41} The first strategy³⁷ is useful for some applications but is not a universal solution, as these oils are incompatible with miscible solvents such as ethanol or methanol, and nonpolar solutes may partition from aqueous droplets into the oil matrix. The second strategy³⁸ is also useful in certain circumstances but is less effective for complex solutions where different protein species may present positive or negative charges at physiological pH. The third strategy³⁹ is useful for preventing cross-contamination (a new film can be used for each experiment) but does not solve the problem of biofouling within a given experiment. The fourth strategy^{40,41} is effective at reducing biofouling, but these surfaces are often difficult to fabricate and cannot tolerate even a small amount of detergent (such as 0.01% Tween 20⁴¹).

We recently developed a general strategy for reducing fouling in DMF, relying on the inclusion of Pluronic additives to droplets used in DMF systems.¹¹ Pluronics are triblock copolymers of poly(ethylene oxide) (PEO) and poly(propylene oxide) (PPO) and are known to reduce protein^{42–44} and cell⁴⁵ adsorption to surfaces. In our initial work,¹¹ we explored the use of two types of Pluronics (Pluronic F68 and Pluronic F127) and demonstrated their capacities to limit protein adsorption and increase device lifetimes. Since that initial report, the pluronic additive strategy has been applied to a diverse range of applications^{14–18,24–26} for digital microfluidics with no indication of adverse effects; for example, the activity of alkaline phosphatase is unaltered even in high concentrations of additive¹⁸ (0.1% Pluronic F127). Of course, there may be applications in which pluronics is problematic; in such cases, the additive may be removed using digital microfluidic solid-phase extraction.⁴⁶

Although pluronic additives have been demonstrated to be useful for digital microfluidics, the recent applications of DMF devices for increasingly complex processes such as cell culture and assays^{14–17} (which necessitate the long-term actuation of solutions containing high concentrations of proteins such as cell culture media and cell lysate) led us to conduct a more exhaustive study to find a better solution for biofouling. Here, we have evaluated eight different Pluronic formulations over a range of concentrations based on their (a) ability to enable the long-term actuation of protein-containing solutions, (b) effects on surface wettabilities, and (c) compatibility with mammalian cell adhesion and proliferation. Our objectives were to discover a superior additive to increase DMF device lifetimes (i.e., to reduce analyte losses during fluid handling and prevent droplet sticking when working with protein solutions), and to characterize the mechanism(s) by which Pluronic additives enable the actuation of protein-containing solutions by DMF. We speculate that this study will be useful for scientists and engineers who are developing digital microfluidic analysis platforms for applications involving protein-containing solutions, and in particular, for applications involving cells.

METHODS AND MATERIALS

Reagents and Materials. Unless specified otherwise, reagents were purchased from Sigma-Aldrich (Oakville, ON). Most Pluronics (BASF Corp., Germany) were generously donated by Brenntag Canada (Toronto, ON); Pluronic F-68 was from Sigma-Aldrich. Parylene-C dimer was obtained from Specialty Coating Systems (Indianapolis, IN). Teflon-AF was from DuPont (Wilmington, DE), and A-174 silane was from GE Silicones (Albany, NY).

Device Fabrication. Digital microfluidic devices were fabricated in the University of Toronto Emerging Communications Technology Institute (ECTI) fabrication facility. Glass substrates bearing patterned chromium electrodes (used as bottom plates of DMF devices) were formed by photolithography and etching as described previously¹⁴ using photomasks printed with 20 000 dpi resolution by Pacific Arts and Design (Toronto, ON). After patterning, the substrates were primed for parylene coating by immersing them in silane solution (2-propanol, DI water, and A-174, 50:50:1 v/v/v) for 15 min, allowing them to air dry and then washing with 2-propanol. After priming, substrates were coated with Parylene-C (6.9 μm) and Teflon-AF (235 nm). Parylene was applied by evaporating 15 g of dimer in a vapor deposition instrument (Specialty Coating Systems), and Teflon-AF was spin-coated (1% in Fluorinert FC-40, 2000 rpm, 60 s) and then postbaked on a hot-plate (160 °C, 10 min). To enable the application of driving potentials, the polymer coatings were locally removed from the contact pads by gentle scraping with a scalpel. Unpatterned top plates were formed by spin-coating indium tin oxide (ITO)-coated glass substrates (Delta Technologies, Stillwater, MN) with Teflon-AF (235 nm, as above).

DMF Device Longevity Analysis. A longevity assay was developed in which droplets of cell culture medium containing Pluronics were actuated across a series of devices, and the number of steps and the time until device failure were recorded for each condition. The details of this assay can be found in Supporting Information.

Contact Angle Measurements. Contact angle measurements were conducted on single-plate DMF devices (i.e., no top-plate) with a single 1×1 cm square electrode. In each experiment, a 4- μL droplet of RPMI 1640 cell culture medium with 10% FBS was positioned on top of the electrode, and the contact angle was measured using the sessile drop fitting method on a Drop Shape Analysis System (Krüss DSA100, Hamburg, Germany). Each droplet contained one of eight Pluronic additives at a concentration ranging from 0 to 0.15% (w/v), and each concentration was evaluated two times on two different devices. In some experiments, the nonpotentiated contact angles (i.e., contact angles of droplets with no potentials applied) were measured every 2.5 min for 20 min. In other experiments, a grounded platinum wire (0.25 mm diameter) was inserted into the top of each droplet, and the electrodynamic contact angles were measured before, during, and 10 s after the application of a 30 s 200 V_{pp} 5 kHz potential. Electrodynamic contact angle hysteresis was defined as the difference between the contact angle observed directly before the application of potential and that observed after the potential is withdrawn (allowing for a few seconds for the droplet to stabilize).

Cell Growth and Viability Assay. Pluronic cytotoxicity experiments were conducted using the Chinese hamster ovary (CHO) cell line. Cells were grown in T-25 flasks in an incubator at 37 °C with 5% CO₂. At the beginning of each experiment, cells were detached using a solution of trypsin (0.25% w/v) and EDTA (1 mM) for 5 min and then centrifuged at 173g for 5 min. The supernatant was removed, and the cells were resuspended at 19 000 cell/cm² in complete cell culture media (50% DMEM, 40% Ham's F12, 10% FBS) containing 0.02% (w/v) Pluronic L62, L64, F68, L92, or P105 and seeded into 24-well plates. The well plates were stored in an incubator at 37 °C with 5% CO₂, and each day, for 3 days, cells were collected (using trypsin/EDTA and washing, as above) from wells and counted using a hemocytometer (Hausser Scientific, Horsham, PA) using the trypan blue exclusion method. Cells were imaged using a Leica DM2000 microscope (Leica Microsystems Canada, Richmond Hill, ON). All cell experiments were conducted in triplicate.

Critical Micelle Concentration Determination. Critical micelle concentrations (CMCs) of Pluronic F68, L92, and P105 in RPMI 1640 cell culture media were determined using the pyrene solubilization method.⁴⁷ Briefly, 10 μL aliquots of 60 μM pyrene in acetone were pipetted into 1.5 mL microcentrifuge tubes, and the acetone was allowed

Table 1. Physical Properties of the Pluronics (PEO_m–PPO_n–PEO_m) Used in This Study

Pluronic	average molecular weight ^d	ave. PPO chain length (<i>n</i>)	ave. PEO chain length (<i>m</i>)	% PEO content	hydrophilic–lipophilic balance (HLB) ^a	CMC in media 25 °C (% wt/v) ^b	batch/lot number ^c
L35	1900	16	11	50	18–23		WPOE579B
F38	4700	16	46	80	>24		WPMD569B
L44	2200	21	11	40	12–18		WPHD524B
L62	2500	30	8	20	1–7		USXW112110
L64	2900	30	13	40	12–18		USXW110132
F68	8400	30	75	80	>24	1.05	097K2410
L92	3650	47	10	20	1–7	0.02	WPIE577B
P105	6500	54	38	50	12–18	0.27	WPIC572B

^a Provided by manufacturer. ^b Critical micelle concentrations in RPMI 1640 cell culture medium were measured using the pyrene solubilization method as described in Methods and Materials. ^c Pluronics were obtained from BASF Corp. (a generous donation from Brenntag Canada), except for F68 which was obtained from Sigma Aldrich.

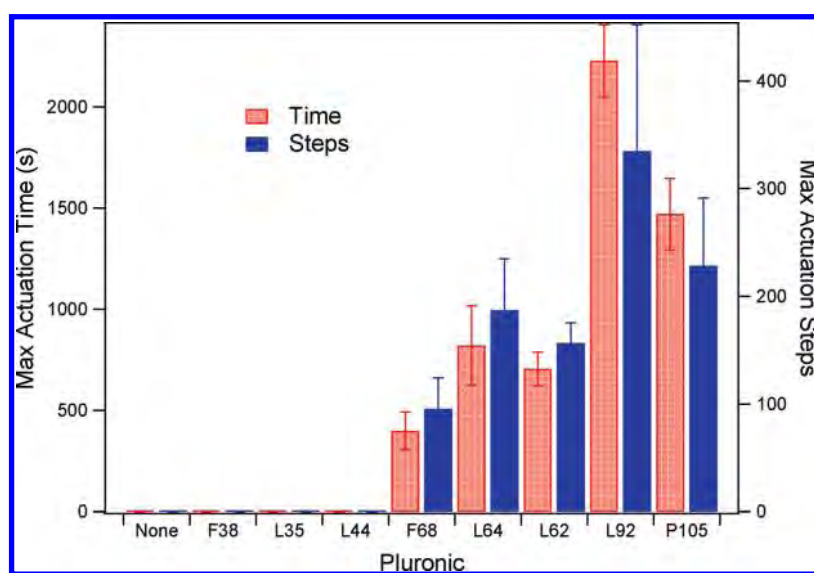


Figure 1. Device longevity assay—initial screen. Droplets containing cell culture media with or without one of eight different Pluronic additives at 0.02% (w/v) were actuated repeatedly across a device until movement failure was observed. The maximum actuation time (left axis) and maximum number of droplet steps (right axis) for the different Pluronics species are arranged (left-to-right) by increasing PPO unit length. Error bars are ± 1 SD.

to evaporate. One milliliter aliquots of media containing 0.005% to 5.0% (w/v) Pluronics were added to each tube such that the final pyrene concentration was 6×10^{-7} M, and the tubes were incubated at 65 °C for 3 h and then at 25 °C overnight. Samples were transferred to quartz cuvettes and analyzed using a Fluoromax-3 fluorescence spectrometer (Horiba Jobin Yvon, Edison, NJ) with excitation at 333 and 339 nm. The ratios of the emission intensities at 380 nm resulting from both excitation wavelengths were used for CMC determination. For dilute solutions of Pluronics, this ratio is independent of concentration, but as the concentrations are raised, the ratio is observed to increase. The Pluronic concentrations at which the ratios begin to increase were taken as the CMCs.⁴⁷ Media without serum was used for these measurements because the serum was found to interfere with the analysis.

Statistical Analysis. Statistical analysis was conducted using JMP Statistical Discovery Software (SAS Institute, Cary, NC). Linear least-squares regression was applied to the maximum time and number of steps as a function of Pluronic molecular weight, PPO chain length, PEO chain length, percent PEO content, hydrophilic–lipophilic balance, initial nonpotentiated contact angle, change in nonpotentiated contact angle over 20 min, contact angle during application of potential, difference in contact angles during and after application of potential, and

difference in contact angles before and after application of potential (i.e., the electrodynamic contact angle hysteresis).

RESULTS AND DISCUSSION

Digital microfluidics (DMF) is a fluid-handling technique in which discrete microdroplets can be dispensed, merged, mixed, and split. As DMF becomes an increasingly popular tool for biological and biochemical applications, methods for reducing biofouling are imminently needed. This is particularly the case for applications involving cells,^{14–17} which often require complex, long-term, and multistep experiments. In a previous study,¹¹ we reported the capacity of two solution additives, Pluronics F68 and Pluronics F127, to reduce the extent of biofouling in digital microfluidics. Pluronics (also known as poloxamers) are PEO and PPO triblock copolymers (PEO_m–PPO_n–PEO_m) with variable PEO and PPO content which dictates the degree of hydrophobicity.

The eight Pluronics species evaluated in this work (L35, F38, L44, L62, L64, F68, L92, and P105), listed in Table 1, were

chosen to cover a wide range of physical and chemical properties. For example, the PPO chain lengths vary from 16 units (L35 and F38) to 54 units (P105), and the PEO content varies from 20% (L62 and L92) to 80% (F38 and F68). For each PEO content percentage, two different PPO lengths were chosen; for example, L62 and L92 each have 20% PEO content but have average PPO lengths of 30 and 47 units, respectively. To identify a strategy for preventing biofouling and to gain a better understanding of the mechanisms behind device fouling, we evaluated the eight different Pluronic over a broad range of concentrations based on their (a) ability to enable the long-term actuation of complex protein-containing solutions by digital microfluidics, (b) effect on droplet wetting, and (c) compatibility with mammalian cellular adhesion and proliferation.

Device Lifetime. Eight species of Pluronic were screened at a concentration of 0.02% (wt/v) for the ability to prolong the motion of droplets of cell culture medium containing 10% fetal bovine serum. This initial concentration of Pluronic (0.02%) was chosen to balance two factors; on one hand, concentrations of 0.05% (F68¹⁶) and 0.08% (F127¹¹) are known to be useful for droplet manipulation in DMF. On the other hand, some Pluronic have been shown to be toxic to cells at moderate-to-high concentrations⁴⁸ that vary depending on which species is used. Thus, 0.02% was used as an initial concentration to balance these two effects, high enough to facilitate droplet movement but low enough to potentially reduce cell toxicity.

The data from the initial screen is shown in Figure 1 and it leads us to three conclusions. First, Pluronic PPO chains must be above a threshold of ~ 30 molecular units to enable motion of droplets of cell culture media containing 10% serum. As shown, droplets failed to move when PPO chain lengths were 21 or less (L44, F38, and F35) (identical to the case in which no additives were present), whereas chain lengths above 30 enabled droplet motion (F64, F68, L62, L92, and P105). Second, the maximum actuation time and the number of successful droplet movement steps before device failure generally increased with increasing PPO chain lengths. Specifically, for a given ratio of PEO to PPO, the longer PPO chain Pluronic had superior droplet movability; for example, L44 (21 PPO units) did not enable droplet motion while L64 (30 PPO units) did. Third, the PPO chain length had a greater influence on droplet movability than percent PEO. For example, for Pluronic with a PPO chain length of 30 molecular units, PEO contents of 20% (L62), 40% (L64), and 80% (F68) all enabled droplet motion. These findings are consistent with literature reports of the importance of longer PPO lengths^{42–44} for reducing protein adsorption to surfaces.

The effects of the two best-performing additives from the initial screen, Pluronic L92 and P105, were then investigated as a function of concentration, along with the previous standard for DMF applications involving cells, F68. As shown in Figure 2, device lifetime was concentration-dependent for all of the Pluronic tested, with optimal concentrations of 0.05%, 0.02%, and 0.02% (wt/v) for F68, L92, and P105, respectively. The condition used previously¹⁶ for manipulation of droplets of cell media, 0.05% Pluronic F68, facilitated a maximum actuation time of 762 ± 162 s. Pluronic L92 at 0.02% enabled actuation for 2227 ± 178 s, and Pluronic P105 at 0.02% enabled actuation for 1470 ± 176 s, both of which were statistically significant improvements over F68 at 0.05% ($p < 0.05$). Interestingly, Pluronic L92 and P105 were most effective at a narrow distribution of concentrations, while Pluronic F68 was effective over a broader range of concentrations.

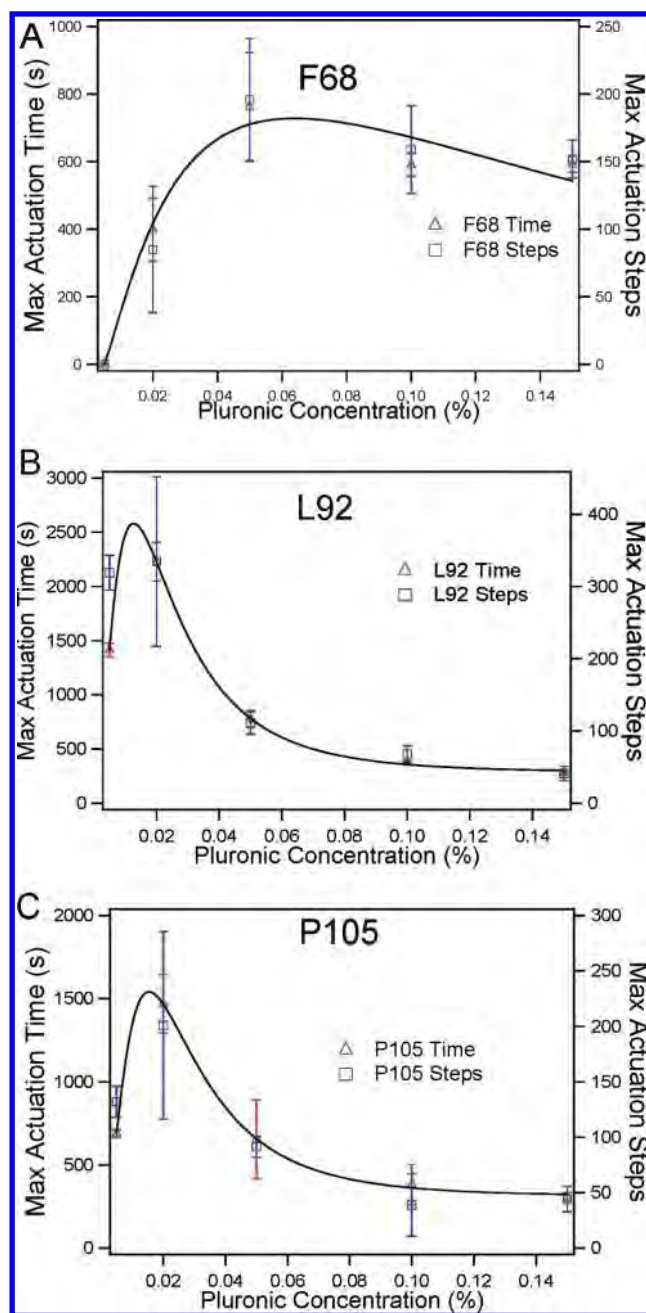


Figure 2. Device longevity assay—concentration dependence. Droplets containing cell culture media with Pluronic F68 (A), L92 (B), and P105 (C) at a range of different concentrations were actuated repeatedly across a device until movement failure was observed, recording the maximum actuation time (left axis) and maximum number of droplet steps (right axis). The maximum actuation time data were fit to log-normal curves. Error bars are ± 1 SD.

Pluronic micelles have been shown to be effective at encapsulating a number of biomolecules.^{49,50} Thus, one possibility for the beneficial effects of Pluronic additives on DMF device longevity is the encapsulation of biomolecules in Pluronic micelles, which may prevent biomolecules from interacting with the device surface. However, the critical micelle concentrations (CMCs) of Pluronic F68, L92, and P105 in media were measured to be 1.05%, 0.02%, and 0.27% (wt/v), respectively. As shown in Figure 2, the concentrations for F68 and L92 which result in

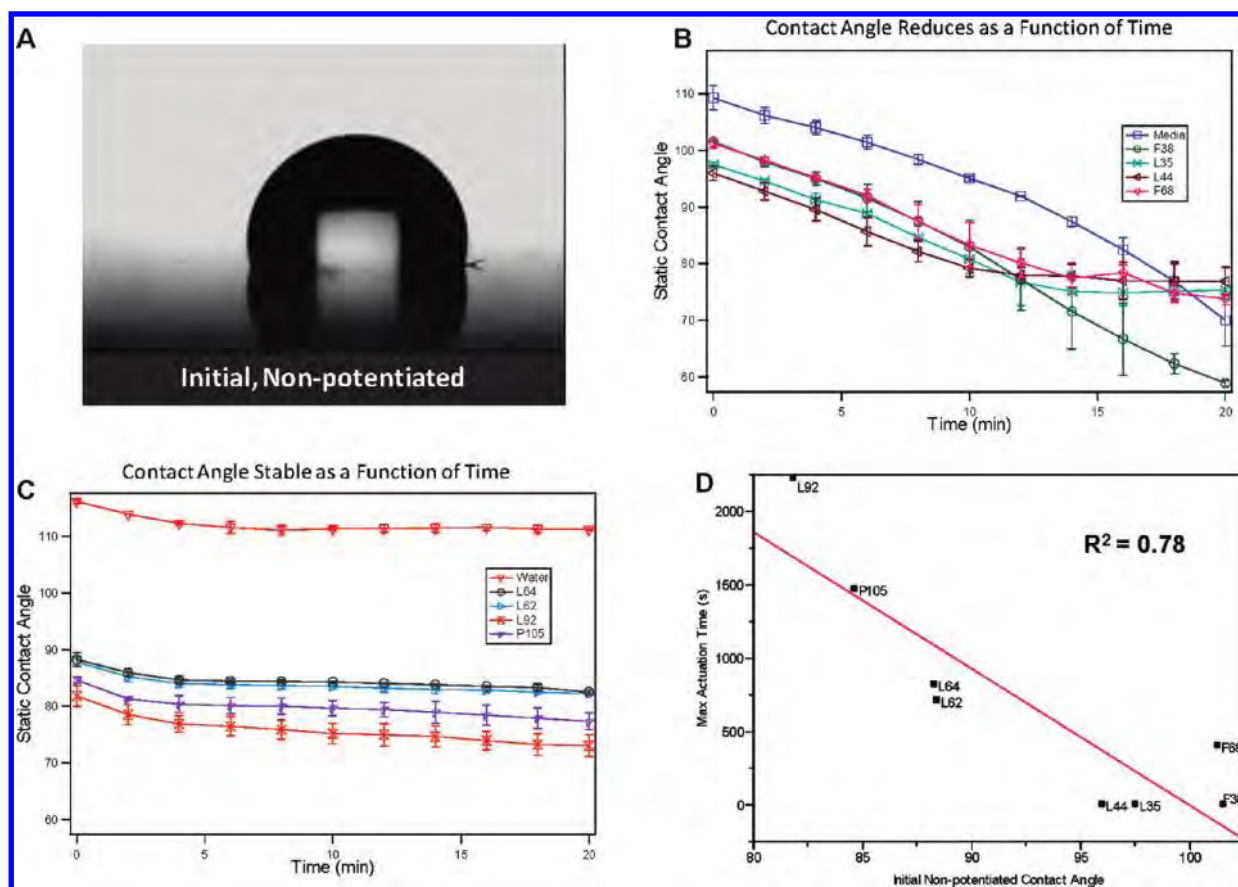


Figure 3. Nonpotentiated contact angles. Picture (A) of a nonpotentiated droplet of cell culture media on a Teflon-AF coated surface. Contact angles of media containing 0.02% (wt/v) Pluronics were measured for 20 min and then categorized as having large changes over time (B) or remaining constant (C). Linear least-squares regression (D) of maximum droplet actuation time (from Figure 1) vs nonpotentiated contact angle ($R^2 = 0.78$). Error bars are ± 1 SD.

maximum device longevity are far lower than the CMCs of these species, which suggests that micelles are not required for improved device performance. Moreover, we propose that the data in Figure 2 suggests that Pluronic–protein interactions (even at sub-CMC concentrations) are unlikely to be the source of the beneficial effects of Pluronic additives on device longevity. We estimate the molar concentration of protein in the experimental system to be 45–68 mM [assuming 3.0–4.5% (wt/v) concentration of protein in serum (as provided by supplier) and 66 kDa average protein molecular weight (of the most abundant protein species, albumin)], while the molar concentrations of Pluronic F68, L92, and P105 in Figure 2 that correlate with the best device performance are estimated to be 60 μM , 55 μM , and 33 μM , respectively (given the average molecular weights listed in Table 1). Thus, there are approximately 3 orders of magnitude more protein molecules than Pluronic molecules in these systems, which suggest that interactions between proteins and pluronic molecules do not explain the observed effects. Rather, we propose that the most likely explanation is that Pluronic molecules form a temporary coating on droplet interfaces, preventing proteins from interacting with the device surfaces. This assertion is supported by the results of Chen et al.,⁵¹ which demonstrated that Pluronic molecules dissolved in aqueous solvents preferentially form dense ordered layers at solution/air and solution/solid interfaces.

Droplet Wetting. After evaluating the effect of Pluronics on device longevity (described above), we evaluated the effects of

the same panel of Pluronic additives on contact angles measured for droplets positioned on device surfaces. We note that this is superficially similar to a wide body of literature^{52–56} from the early 2000s that sought to model digital microfluidics in terms of “electrowetting”, i.e., the reduction in contact angle of a droplet upon application of an external electrical field. We are skeptical of electrowetting as a fluid manipulation model, given that liquids with no electrowetting behavior are movable on digital microfluidic devices.⁵⁷ Thus, the contact angle measurements presented here were not used to explore the mechanism of droplet movement but rather to probe the nature of the effects of Pluronic additives on protein adsorption to surfaces.

As a first step, the contact angles were measured for droplets of cell culture media with 10% fetal bovine serum containing 0.02% (wt/v) of each of the eight different Pluronic additives in a nonpotentiated state (i.e., with no voltage applied). A representative picture of such a droplet is shown in Figure 3A. Upon observation of the results, the additives were categorized into two classes. (1) In some cases (Figure 3B), droplet contact angles decrease as a function of time. This behavior is typified by media not containing any additives (blue squares in Figure 3B) and is likely an effect of protein adsorption to the surface as time progresses; as more protein adsorbs, the surface becomes more hydrophilic, resulting in lower contact angles. Interestingly, the additives that exhibit this behavior (with decreasing contact angles as a function of time) were incapable of supporting droplet

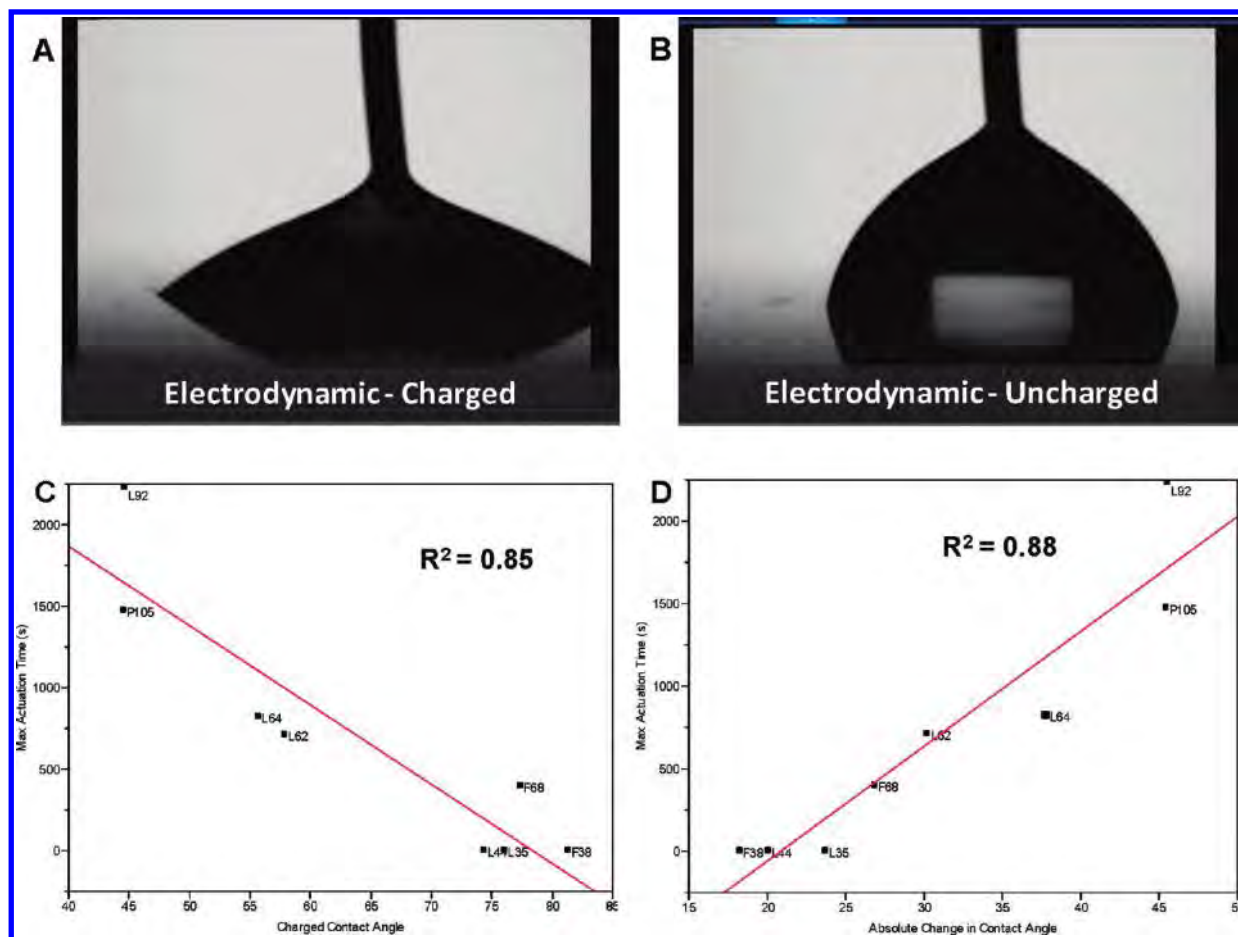


Figure 4. Electrodynamic contact angles. Pictures of droplets on a device during (A) and after removal (B) application of a 200 V_{PP} potential. Linear least-squares regression of maximum droplet actuation time (from Figure 1) vs electrodynamic contact angle during charging ($R^2 = 0.85$) (C) and vs the difference in contact angle between the charged to decharged states ($R^2 = 0.88$) (D).

movement (see Figure 1) with one exception: Pluronic F68. (2) In other cases (Figure 3C), droplet contact angles are fairly constant as a function of time. This behavior is typified by liquids not containing any proteins, such as DI water (red upside-down triangles in Figure 3C). We propose that the additives that facilitate this behavior (L64, L62, L92, and P105) for protein-containing solutions are effective at preventing protein adsorption on this time scale. Note that the two behaviors (reducing contact angle vs constant contact angle as a function of time) correlate approximately with PPO chain length. With the exception of Pluronic F68, the additives in Figure 3B have PPO chain lengths <30, and the additives in Figure 3C have chain lengths ≥ 30 .

The nonpotentiated contact angle data in Figure 3B and 3C show another trend. Immediately after deposition of the droplet on the surface, the nonpotentiated contact angles were lower for additives in Figure 3C than for the additives in Figure 3B. This is a useful observation, which we propose may be useful for screening additives for utility for digital microfluidics. In fact, when examined quantitatively, there is an inverse correlation ($R^2 = 0.78$) between maximum actuation time on DMF devices (from Figure 1) and the initial nonpotentiated contact angle, which is plotted in Figure 3D. For example, the two Pluronic additives which enabled the longest lifetimes were L92 and P105 (from Figure 1), and these additives were observed to have the lowest initial nonpotentiated

contact angles of 82° and 85° . It is likely that the primary reason for droplet movement failure in the device longevity assay is the adsorption of proteins to the device surface. Under this assumption, the data in Figure 3D suggests that the more attracted the Pluronic molecules are to the surface (resulting in lower initial contact angles), the greater the extent of protection of the surface from protein adsorption. This finding is consistent with literature on the influence of wettability on protein adsorption; in general, lower contact angles for aqueous droplets on uncharged surfaces are known to be associated with reduced protein adhesion.^{58–60} Pluronics with longer PPO chains assemble more readily on hydrophobic device surfaces and also are more difficult to displace once assembled.^{61,62} Both of these phenomena are likely to be useful for preventing protein adsorption on DMF device surfaces.

After evaluating the relationship between nonpotentiated contact angle and device longevity, we turned our attention to electrodynamic contact angles. In DMF devices, when an aqueous droplet positioned on an insulator is positioned over a charged electrode (i.e., with potential applied), the droplet is observed to assume a wetted geometry (Figure 4A). When the electrical potential is then removed, the droplet is observed to recover to a nonwetted geometry on the now decharged electrode (Figure 4B). The electrodynamic contact angles were measured for the series of cell culture media formulations containing

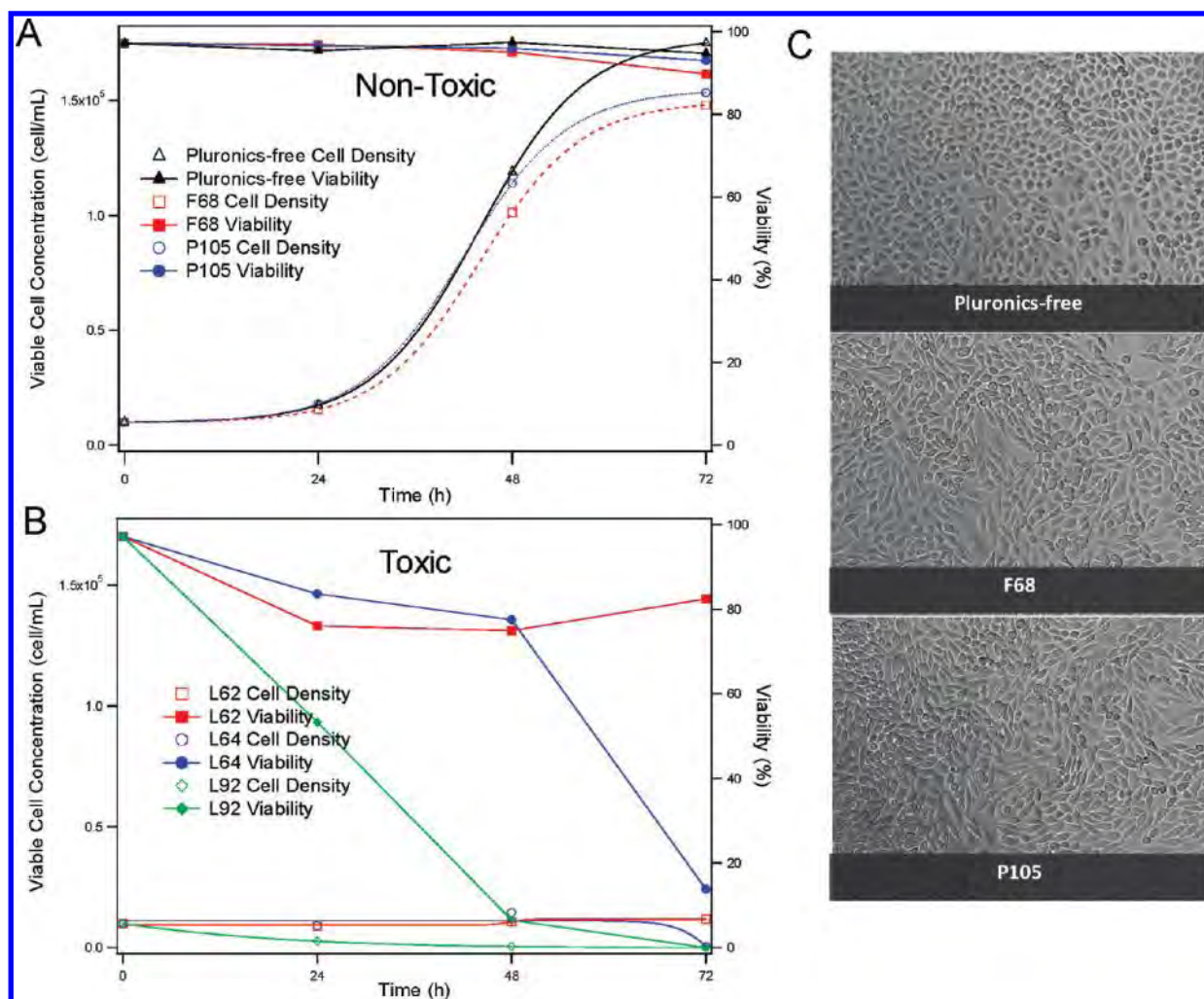


Figure 5. Cell compatibility. Viability (right axes) and density (left axes) of CHO cells cultured over 3 days without Pluronic, in Pluronic F68 and P105 at 0.02% (wt/v) (A) and in Pluronic L62, L64, and L92 at 0.02% (wt/v) (B). Photomicrographs for CHO cells after 3 days cultured Pluronic-free, in 0.02% F68 and 0.02% P105 (C). Cells show comparable growth rates and morphologies in the presence of F68 and P105 to standard Pluronic-free conditions.

Pluronic; as far as we are aware, this is the first time electrodynamic contact angles have been measured for Pluronic-containing liquids. As was the case for nonpotentiated contact angles, there was a strong inverse correlation ($R^2 = 0.85$) between maximum actuation time on DMF devices (from Figure 1) and charged contact angle, which is plotted in Figure 4C. For example, the Pluronic additives with the most beneficial effects on device longevity, L92 and P105, had the lowest charged contact angles of 44.6° and 44.5° . Moreover, there was an even stronger correlation ($R^2 = 0.88$) between the maximum actuation time on DMF devices and the change in contact angles between the charged and discharged states, which is shown in Figure 4D. Again, L92 and P105 had the highest observed contact angle changes of 45.5° and 45.4° . Interestingly, no correlations were found between electrodynamic contact angle hysteresis (i.e., the difference between nonpotentiated contact angles measured before and after charging the electrode) and maximum actuation time or PPO/PEO chain lengths. Regardless, the contact angle results presented in Figures 3 and 4 are useful predictors of the effects of additives on device lifetime, and we suggest that future investigation of new additives may want to use similar measurements as a screen for beneficial effects.

Compatibility with Cell Culture. A primary goal for this work was to identify Pluronic additives that do not interfere with cell culture. To this end, Chinese hamster ovary (CHO) cells were cultured for 3 days in the presence of the five best performing Pluronic species from the initial screens at concentrations of 0.02% (wt/v) to characterize their effects on viability (as a marker for toxicity) and cell density (as a marker for effects on proliferation). Upon observation of the results, the five additives were categorized into two classes, nontoxic and toxic, and the data are summarized in Figure 5. As shown, Pluronic F68 and P105 were found to be nontoxic to CHO cells and had little or no effect on proliferation (Figure 5A). Moreover, as shown in Figure 5C, these two additives had little or no impact on cell morphology or adhesion to the substrates. In contrast, Pluronic L62, L64, and L92 had significant cytotoxicity (with viabilities decreasing to less than 20% within 3 days) and in addition prevented cell proliferation (Figure 5B). This observation is supported by previous work⁴⁸ in which Pluronic L64 was found to be cytotoxic to epithelial cell lines and primary macrophages *in vitro*. Interestingly, the Pluronic species categorized as non toxic had higher PEO content (50% or higher) and higher hydrophilic–lipophilic balance (HLB) values than the species

categorized as toxic (Table 1). We speculate that the more lipophilic Pluronics (with lower HLB) are more likely to interact with and disrupt phospholipid bilayers, compromising cell membrane integrity. It is clear that Pluronics P105 and F68 at 0.02% are not detrimental to CHO cells. It is reasonable to assume that many immortalized cell lines will fare similarly, but we caution that cell phenotypes vary considerably, so effects should be tested before use.

CONCLUSIONS

We evaluated a series of Pluronic block copolymers as additives for use with digital microfluidics to reduce protein adsorption and prolong device lifetime. Of the formulations tested (which included Pluronics F68, which has been used extensively for this purpose), the additives that yielded the best device performance were Pluronics L92 and P105 at 0.02% (wt/v). For applications involving mammalian cells, however, P105 is a better choice, as L92 is cytotoxic to Chinese hamster ovary cells at 0.02%. More generally, when selecting Pluronic additives to improve device longevity in DMF devices, we recommend that Pluronic species should have long PPO chain lengths (30 units or greater). For use with cells, greater PEO content (50% or more) is likely to be important. To this end, Pluronic species such as F88 and F108 (which were not evaluated here) are likely good candidates because they have high PEO content and PPO chain lengths within the acceptable range determined in this study. It is important to note that concentration dependence should be evaluated for any future Pluronic additive candidates because droplet movability is highly dose-dependent. Finally, if full device longevity assays cannot be performed (as may be the case if a large matrix of conditions is being evaluated), we recommend that contact angles may be a useful screen; lower initial non-potentialized and electrodynamic/charged contact angles, and higher contact angle differences between charged and discharged states, correlate with improved performance on the device. As we advance our understanding of the mechanisms behind biofouling and biofouling prevention in digital microfluidic devices, we will greatly increase its suitability for an ever-greater range of applications.

ASSOCIATED CONTENT

S Supporting Information. Additional information as noted in the text. This material is available free of charge via the Internet at <http://pubs.acs.org>.

AUTHOR INFORMATION

Corresponding Author

*E-mail: aaron.wheeler@utoronto.ca. Tel: (416) 946 3864. Fax: (416) 946 3865.

ACKNOWLEDGMENT

We thank Professor Warren Chan (IBBME, University of Toronto, Canada) for use of the UV-vis spectrometer and Professor Eugenia Kumacheva (Department of Chemistry, University of Toronto) for use of the contact angle goniometer. We thank the Canadian Institutes for Health Research (CIHR) for financial support. S.H.A. thanks the National Sciences and Engineering Research Council (NSERC) for a graduate fellowship, and A.R.W. thanks the Canada Research Chair (CRC) Program for a CRC.

REFERENCES

- (1) Le-Clech, P.; Chen, V.; Fane, T. A. G. Fouling in membrane bioreactors used in wastewater treatment. *J. Membr. Sci.* **2006**, *284* (1–2), 17–53.
- (2) Nystrom, M.; Kaipia, L.; Luque, S. Fouling and retention of nanofiltration membranes. *J. Membr. Sci.* **1995**, *98* (3), 249–262.
- (3) Morra, M. On the molecular basis of fouling resistance. *J. Biomater. Sci., Polym. Ed.* **2000**, *11* (6), 547–569.
- (4) Mukhopadhyay, R. When microfluidic devices go bad - How does fouling occur in microfluidic devices, and what can be done about it? *Anal. Chem.* **2005**, *77* (21), 429A–432A.
- (5) Wahlgren, M.; Arnebrant, T. Protein adsorption to solid-surfaces. *Trends Biotechnol.* **1991**, *9* (6), 201–208.
- (6) Khademhosseini, A.; Suh, K. Y.; Jon, S.; Eng, G.; Yeh, J.; Chen, G. J.; Langer, R. A soft lithographic approach to fabricate patterned microfluidic channels. *Anal. Chem.* **2004**, *76* (13), 3675–3681.
- (7) Papat, K. C.; Desai, T. A. Poly(ethylene glycol) interfaces: an approach for enhanced performance of microfluidic systems. *Biosens. Bioelectron.* **2004**, *19* (9), 1037–1044.
- (8) Linder, V.; Verpoorte, E.; Thormann, W.; de Rooij, N. F.; Sigrist, M. Surface biopassivation of replicated poly(dimethylsiloxane) microfluidic channels and application to heterogeneous immunoreaction with on-chip fluorescence detection. *Anal. Chem.* **2001**, *73* (17), 4181–4189.
- (9) Hu, S. W.; Ren, X. Q.; Bachman, M.; Sims, C. E.; Li, G. P.; Allbritton, N. Surface modification of poly(dimethylsiloxane) microfluidic devices by ultraviolet polymer grafting. *Anal. Chem.* **2002**, *74* (16), 4117–4123.
- (10) Vlachopoulou, M. E.; Petrou, P. S.; Kakabakos, S. E.; Tserepi, A.; Beltsios, K.; Gogolides, E. Effect of surface nanostructuring of PDMS on wetting properties, hydrophobic recovery and protein adsorption. *Microelectron. Eng.* **2009**, *86* (4–6), 1321–1324.
- (11) Luk, V. N.; Mo, G.; Wheeler, A. R. Pluronic additives: a solution to sticky problems in digital microfluidics. *Langmuir* **2008**, *24* (12), 6382–9.
- (12) Wheeler, A. R. Chemistry. Putting electrowetting to work. *Science* **2008**, *322* (5901), 539–40.
- (13) Jebail, M. J.; Wheeler, A. R. Let's get digital: digitizing chemical biology with microfluidics. *Curr. Opin. Chem. Biol.* **2010**, *14* (5), 574–581.
- (14) Barbulovic-Nad, I.; Yang, H.; Park, P. S.; Wheeler, A. R. Digital microfluidics for cell-based assays. *Lab Chip* **2008**, *8* (4), 519–26.
- (15) Shah, G. J.; Ohta, A. T.; Chiou, E. P.; Wu, M. C.; Kim, C. J. EWOD-driven droplet microfluidic device integrated with optoelectronic tweezers as an automated platform for cellular isolation and analysis. *Lab Chip* **2009**, *9* (12), 1732–9.
- (16) Barbulovic-Nad, I.; Au, S. H.; Wheeler, A. R. A microfluidic platform for complete mammalian cell culture. *Lab Chip* **2010**, *10* (12), 1536–1542.
- (17) Au, S. H. S.; Wheeler, A. R. Integrated Microbioreactor for Culture and Analysis of Bacteria, Algae and Yeast. *Biomed. Micro-devices* **2011**, *13*, 41–50.
- (18) Miller, E. M.; Wheeler, A. R. A digital microfluidic approach to homogeneous enzyme assays. *Anal. Chem.* **2008**, *80* (5), 1614–1619.
- (19) Srinivasan, V.; Pamula, V. K.; Fair, R. B. Droplet-based microfluidic lab-on-a-chip for glucose detection. *Anal. Chim. Acta* **2004**, *507* (1), 145–150.
- (20) Srinivasan, V.; Pamula, V. K.; Fair, R. B. An integrated digital microfluidic lab-on-a-chip for clinical diagnostics on human physiological fluids. *Lab Chip* **2004**, *4* (4), 310–315.
- (21) Martin, J. G.; Gupta, M.; Xu, Y. M.; Akella, S.; Liu, J.; Dordick, J. S.; Linhardt, R. J. Toward an Artificial Golgi: Redesigning the Biological Activities of Heparan Sulfate on a Digital Microfluidic Chip. *J. Am. Chem. Soc.* **2009**, *131* (31), 11041–11048.
- (22) Sista, R.; Hua, Z.; Thwar, P.; Sudarsan, A.; Srinivasan, V.; Eckhardt, A.; Pollack, M.; Pamula, V. Development of a digital microfluidic platform for point of care testing. *Lab Chip* **2008**, *8* (12), 2091–104.
- (23) Sista, R. S.; Eckhardt, A. E.; Srinivasan, V.; Pollack, M. G.; Palanki, S.; Pamula, V. K. Heterogeneous immunoassays using magnetic

beads on a digital microfluidic platform. *Lab Chip* **2008**, *8* (12), 2188–96.

(24) Miller, E. M.; Ng, A. H. C.; Uddayasankar, U.; Wheeler, A. R. A Digital Microfluidic Approach to Heterogeneous Immunoassays. *Anal. Bioanal. Chem.* **2010**, *339*, 337–345.

(25) Jebrail, M. J.; Wheeler, A. R. Digital microfluidic method for protein extraction by precipitation. *Anal. Chem.* **2009**, *81* (1), 330–5.

(26) Luk, V. N.; Wheeler, A. R. A Digital Microfluidic Approach to Proteomic Sample Processing. *Anal. Chem.* **2009**, *81* (11), 4524–4530.

(27) Moon, H.; Wheeler, A. R.; Garrell, R. L.; Loo, J. A.; Kim, C. J. An integrated digital microfluidic chip for multiplexed proteomic sample preparation and analysis by MALDI-MS. *Lab Chip* **2006**, *6* (9), 1213–1219.

(28) Wheeler, A. R.; Moon, H.; Bird, C. A.; Loo, R. R. O.; Kim, C. J.; Loo, J. A.; Garrell, R. L. Digital microfluidics with in-line sample purification for proteomics analyses with MALDI-MS. *Anal. Chem.* **2005**, *77* (2), 534–540.

(29) Jebrail, M. J.; Luk, V. N.; Shih, S. C. C.; Fobel, R.; Ng, A.; Yang, H.; Freire, S. L. S.; Wheeler, A. R. Digital Microfluidics for Automated Proteomic Processing. *J. Visualized Experiments* **2009**, *6* (33), 1603.

(30) Chatterjee, D.; Ytterberg, A. J.; Son, S. U.; Loo, J. A.; Garrell, R. L. Integration of Protein Processing Steps on a Droplet Microfluidics Platform for MALDI-MS Analysis. *Anal. Chem.* **2010**, *82* (5), 2095–2101.

(31) Malic, L.; Brassard, D.; Veres, T.; Tabrizian, M. Integration and detection of biochemical assays in digital microfluidic LOC devices. *Lab Chip* **2010**, *10* (4), 418–431.

(32) Hua, Z. S.; Rouse, J. L.; Eckhardt, A. E.; Srinivasan, V.; Pamula, V. K.; Schell, W. A.; Benton, J. L.; Mitchell, T. G.; Pollack, M. G. Multiplexed Real-Time Polymerase Chain Reaction on a Digital Microfluidic Platform. *Anal. Chem.* **2010**, *82* (6), 2310–2316.

(33) Chang, Y. H.; Lee, G. B.; Huang, F. C.; Chen, Y. Y.; Lin, J. L. Integrated polymerase chain reaction chips utilizing digital microfluidics. *Biomed. Microdevices* **2006**, *8* (3), 215–225.

(34) Mousa, N. A.; Jebrail, M. J.; Yang, H.; Abdegawad, M.; Metalnikov, P.; Chen, J.; Wheeler, A. R.; Casper, R. F. Droplet-Scale Estrogen Assays in Breast Tissue, Blood, and Serum. *Sci. Transl. Med.* **2009**, *1* (1), 1ra2.

(35) Lumsdon, S. O.; Green, J.; Stieglitz, B. Adsorption of hydrophobin proteins at hydrophobic and hydrophilic interfaces. *Colloids Surf., B* **2005**, *44* (4), 172–178.

(36) Vermeer, A. W. P.; Giacomelli, C. E.; Norde, W. Adsorption of IgG onto hydrophobic Teflon. Differences between the F-ab and F-c domains. *Biochim. Biophys. Acta* **2001**, *1526* (1), 61–69.

(37) Srinivasan, V.; Pamula, V. K.; Fair, R. B. An integrated digital microfluidic lab-on-a-chip for clinical diagnostics on human physiological fluids. *Lab Chip* **2004**, *4* (4), 310–5.

(38) Yoon, J. Y.; Garrell, R. L. Preventing biomolecular adsorption in electrowetting-based biofluidic chips. *Anal. Chem.* **2003**, *75* (19), 5097–5102.

(39) Yang, H.; Luk, V. N.; Abdegawad, M.; Barbulovic-Nad, I.; Wheeler, A. R. A world-to-chip interface for digital microfluidics. *Anal. Chem.* **2009**, *81* (3), 1061–7.

(40) Koc, Y.; de Mello, A. J.; McHale, G.; Newton, M. I.; Roach, P.; Shirtcliffe, N. J. Nano-scale superhydrophobicity: suppression of protein adsorption and promotion of flow-induced detachment. *Lab Chip* **2008**, *8* (4), 582–586.

(41) Jonsson-Niedziolka, M.; Lapierre, F.; Coffinier, Y.; Parry, S. J.; Zoueshtiagh, F.; Foat, T.; Thomy, V.; Boukherroub, R. EWOD driven cleaning of bioparticles on hydrophobic and superhydrophobic surfaces. *Lab Chip* **2011**, *11* (3), 490–496.

(42) Green, R. J.; Davies, M. C.; Roberts, C. J.; Tendler, S. J. B. A surface plasmon resonance study of albumin adsorption to PEO-PPO-PEO triblock copolymers. *J. Biomed. Mater. Res.* **1998**, *42* (2), 165–171.

(43) Green, R. J.; Tasker, S.; Davies, J.; Davies, M. C.; Roberts, C. J.; Tendler, S. J. B. Adsorption of PEO-PPO-PEO Triblock Copolymers at the Solid/Liquid Interface: A Surface Plasmon Resonance Study. *Langmuir* **1997**, *13* (24), 6510–6515.

(44) Amiji, M.; Park, K. Prevention of protein adsorption and platelet-adhesion on surfaces by PEO PPO PEO triblock copolymers. *Biomaterials* **1992**, *13* (10), 682–692.

(45) McClain, M. A.; Culbertson, C. T.; Jacobson, S. C.; Allbritton, N. L.; Sims, C. E.; Ramsey, J. M. Microfluidic Devices for the High-Throughput Chemical Analysis of Cells. *Anal. Chem.* **2003**, *75* (21), 5646–5655.

(46) Yang, H.; Mudrik, J. M.; Jebrail, M. J.; Wheeler, A. R. A Digital Microfluidic Method for in Situ Formation of Porous Polymer Monoliths with Application to Solid-Phase Extraction. *Anal. Chem.* **2011**, *83* (10), 3824–3830.

(47) Wilhelm, M.; Zhao, C. L.; Wang, Y. C.; Xu, R. L.; Winnik, M. A.; Mura, J. L.; Riess, G.; Croucher, M. D. Polymer micelle formation 0.3. poly(styrene-ethylene oxide) block copolymer micelle formation in water - a fluorescence probe study. *Macromolecules* **1991**, *24* (5), 1033–1040.

(48) Kier, L. D.; Wagner, L. M.; Wilson, T. V.; Li, A. P.; Short, R. D.; Kennedy, G. L. Cytotoxicity of ethylene oxide/propylene oxide copolymers in cultured-mammalian-cells. *Drug Chem. Toxicol.* **1995**, *18* (1), 29–41.

(49) Kabanov, A. V.; Batrakova, E. V.; Alakhov, V. Y. Pluronic (R) block copolymers as novel polymer therapeutics for drug and gene delivery. *J. Controlled Release* **2002**, *82* (2–3), 189–212.

(50) Choi, J. H.; Jang, J. Y.; Joung, Y. K.; Kwon, M. H.; Park, K. D., Intracellular delivery and anti-cancer effect of self-assembled heparin-Pluronic nanogels with RNase A. *J. Controlled Release* **2010**, *147* (3), 420–427.

(51) Chen, C. Y.; Even, M. A.; Chen, Z. Detecting molecular-level chemical structure and group orientation of amphiphilic PEO-PPO-PEO copolymers at solution/air and solid/solution interfaces by SFG vibrational spectroscopy. *Macromolecules* **2003**, *36* (12), 4478–4484.

(52) Lee, J.; Moon, H.; Fowler, J.; Schoellhammer, T.; Kim, C. J. Electrowetting and electrowetting-on-dielectric for microscale liquid handling. *Sens. Actuators, A* **2002**, *95* (2–3), 259–268.

(53) Cho, S. K.; Moon, H. J.; Kim, C. J. Creating, transporting, cutting, and merging liquid droplets by electrowetting-based actuation for digital microfluidic circuits. *J. Microelectromech. Syst.* **2003**, *12* (1), 70–80.

(54) Moon, H.; Cho, S. K.; Garrell, R. L.; Kim, C. J. Low voltage electrowetting-on-dielectric. *J. Appl. Phys.* **2002**, *92* (7), 4080–4087.

(55) Pollack, M. G.; Fair, R. B.; Shenderov, A. D. Electrowetting-based actuation of liquid droplets for microfluidic applications. *Appl. Phys. Lett.* **2000**, *77* (11), 1725–1726.

(56) Pollack, M. G.; Shenderov, A. D.; Fair, R. B. Electrowetting-based actuation of droplets for integrated microfluidics. *Lab Chip* **2002**, *2* (2), 96–101.

(57) Chatterjee, D.; Hetayothin, B.; Wheeler, A. R.; King, D. J.; Garrell, R. L. Droplet-based microfluidics with nonaqueous solvents and solutions. *Lab Chip* **2006**, *6* (2), 199–206.

(58) Sigal, G. B.; Mrksich, M.; Whitesides, G. M. Effect of surface wettability on the adsorption of proteins and detergents. *J. Am. Chem. Soc.* **1998**, *120* (14), 3464–3473.

(59) Sethuraman, A.; Han, M.; Kane, R. S.; Belfort, G. Effect of surface wettability on the adhesion of proteins. *Langmuir* **2004**, *20* (18), 7779–7788.

(60) Elwing, H.; Welin, S.; Askendal, A.; Nilsson, U.; Lundstrom, I. A wettability gradient-method for studies of macromolecular interactions at the liquid solid interface. *J. Colloid Interface Sci.* **1987**, *119* (1), 203–210.

(61) Andrade, J.; Hlady, V. Protein adsorption and materials biocompatibility: A tutorial review and suggested hypotheses. In *Biopolymers/Non-Exclusion HPLC*; Springer: Heidelberg, Germany, 1986; pp 1–63.

(62) Lee, J. H.; Lee, H. B.; Andrade, J. D. Blood compatibility of polyethylene oxide surfaces. *Prog. Polym. Sci.* **1995**, *20* (6), 1043–1079.